Lasers Med Sci (2017) 32:1309–1320
DOI 10.1007/s10103-017-2243-5

ORIGINAL ARTICLE

Mesenchymal stromal cell and osteoblast responses to oxidized titanium surfaces pre-treated with λ = 808 nm GaAlAs diode laser or chlorhexidine: in vitro study

Flaminia Chellini[1] · Marco Giannelli[2] · Alessia Tani[1] · Lara Ballerini[3] · Larissa Vallone[1] · Daniele Nosi[1] · Sandra Zecchi-Orlandini[1] · Chiara Sassoli[1]

Received: 7 December 2016 / Accepted: 19 May 2017 / Published online: 27 May 2017

Abstract Preservation of implant biocompatibility following peri-implantitis treatments is a crucial issue in odontostomatological practice, being closely linked to implant re-osseointegration. Our aim was to assess the responses of osteoblast-like Saos2 cells and adult human bone marrow-mesenchymal stromal cells (MSCs) to oxidized titanium surfaces (TiUnite®, TiU) pre-treated with a 808 ± 10 nm GaAlAs diode laser operating in non-contact mode, in continuous (2 W, 400 J/cm^2; CW) or pulsed (20 kHz, 7 μs, 0.44 W, 88 J/cm^2; PW) wave, previously demonstrated to have a strong bactericidal effect and proposed as optional treatment for peri-implantitis. The biocompatibility of TiU surfaces pre-treated with chlorhexidine digluconate (CHX) was also evaluated. In particular, in order to mimic the in vivo approach, TiU surfaces were pre-treated with CHX (0.2%, 5 min); CHX and rinse; and CHX, rinse and air drying. In some experiments, the cells were cultured on untreated TiU before being exposed to CHX. Cell viability (MTS assay), proliferation (EdU incorporation assay; Ki67 confocal immunofluorescence analysis), adhesion (morphological analysis of actin cytoskeleton organization), and osteogenic differentiation (osteopontin confocal immunofluorescence analysis; mineralized bone-like nodule formation) analyses were performed. CHX resulted cytotoxic in all experimental conditions. Diode laser irradiation preserved TiU surface biocompatibility. Notably, laser treatment appeared even to improve the known osteoconductive properties of TiU surfaces. Within the limitations of an in vitro experimentation, this study contributes to provide additional experimental basis to support the potential use of 808 ± 10 nm GaAlAs diode laser at the indicated irradiation setting, in the treatment of peri-implantitis and to discourage the use of CHX.

Keywords Osteoblasts · Mesenchymal stromal cells · Titanium dental implant · Diode laser therapy · Peri-implantitis · Chlorhexidine

✉ Chiara Sassoli
chiara.sassoli@unifi.it

[1] Department of Experimental and Clinical Medicine—Section of Anatomy and Histology, University of Florence, Largo Brambilla 3, 50134 Florence, Italy

[2] Odontostomatologic Laser Therapy Center, Via dell' Olivuzzo 162, 50143 Florence, Italy

[3] Department of Experimental and Clinical Medicine—Section of Haematology, University of Florence, Largo Brambilla 3, 50134 Florence, Italy

Introduction

Dental implant therapy represents nowadays the treatment of choice for edentulous patients, which allows restoration of the masticatory function and esthetics with satisfactory and often spectacular outcomes. However, although the development of new implant surfaces and the number of placed implants continue to increase, their use is still associated with the onset of some complications, including peri-implantitis [1]. This pathological condition represents the most important local inflammatory disease of the hard and soft tissues supporting dental implants, mainly caused by peri-odontopathogenic bacteria accumulating on implant surface, which may lead, if not treated, to bone loss and, ultimately, to implant failure [2]. It is well established that bacteria and bacterial toxin eradication from implant surfaces represents a pre-requisite to arrest the progression of peri-implantitis and to allow the restoration of the bone tissue surrounding the previously infected implant [3, 4].

Numerous studies have investigated the efficacy of different implant decontamination procedures, including air-

powered, chemical methods; mechanical cleaning with metal and plastic curettes; or ultrasonic scalers and laser therapy, but no gold standard has been proposed yet to this purpose. Moreover, there is still a lack of information about how these treatments impact on the biocompatibility of the dental implant surface with the cells of peri-implant tissues [3–8]. Among different treatments, laser therapy has been recently suggested as the most innovative and promising therapeutic option especially in view of the powerful anti-microbial effect of laser light [6, 9, 10]. However, at present, univocal guidelines for its use for dental implant bacterial decontamination in the peri-implantitis treatment are not available. This is mainly due to the complexity of medical lasers in terms of type, energy output modes, and setting parameters which has produced a multiplicity of protocols with totally different outcomes, thus hampering the evaluation and comparison of the results [11, 12]. Moreover, little is still known concerning the effects of laser irradiation on implant surfaces in terms of thermal effect and modifications of their physical, mechanical, and chemical properties [13]. The knowledge of these effects is critical for every clinician who wants to perform a laser treatment on dental implants. In fact, the physical and chemical characteristics of each implant surface lead to substantial differences in their laser energy absorption/reflection features and hence susceptibility to heating and to heat-induced damage on surrounding soft and hard tissues [14, 15]. In addition, topographical configuration, geometry, and chemical composition of implant surface have been demonstrated to influence the initial response of the cells involved in bone formation, namely mesenchymal cells and osteoblasts at the cell-material interface. This can in turn affect the rate and quality of the newly formed bone tissue and therefore the bone-to-implant anchorage (osseointegration and re-osseointegration) which is mandatory for implant long-term success [16–18]. Diode lasers are widely used in periodontics and have been reported to perform effective implant surface decontamination [19, 20]. In line with this, we have recently demonstrated that irradiation with a 808 ± 10 nm GaAlAs diode laser, set at 2 W output energy in continuous (2 W, 400 J/cm^2) or pulsed (20 kHz, 7 μs, 0.44 W, 88 J/cm^2) wave operating in a non-contact mode with an airflow cooling system, can achieve the decontamination of *Staphylococcus aureus* biofilm and detoxification of *Escherichia coli* lipopolysaccharide on commercially used TiUnite® dental implants (Nobel Biocare, Göteborg, Sweden) while maintaining the disc temperature below the tissue damage threshold and without inducing any morphological alterations of the implant surface [14, 21]. TiUnite®, corresponding to the osseous interface of the implant, is titanium oxide (TiO_2), rendered into a porous osteoconductive biomaterial through spark anodization, to hasten osseointegration [17, 18, 22].

On such premises, the present in vitro study is aimed to extend the knowledge on the effects of 808 ± 10 nm GaAlAs diode laser irradiation (with the same parameters as above) of TiUnite® surfaces, by evaluating its impact on the implant biocompatibility with osteoblasts and mesenchymal stromal cells (MSCs) (i.e., cell viability, proliferation, adhesion, and osteogenic differentiation). In parallel, we evaluated also the biocompatibility of TiUnite® surfaces treated with one of the most frequently used implant chemical decontaminating agents such as chlorhexidine digluconate [23, 24].

Material and methods

Oxidized titanium discs

The experiments were performed on 6 mm in diameter, 2-mm-thick oxidized titanium discs with the same chemical composition and physical characteristics of the commercial TiUnite® dental implants (TiU, Nobel Biocare, Göteborg, Sweden) as described in detail previously [14]. Before using, the discs were ultrasonically cleaned in acetone, rinsed in distilled water, and autoclaved (120 °C for 15 min).

808 ± 10 nm GaAlAs diode laser treatment

The laser treatment with diode GaAlAs laser emitting at λ = 808 ± 10 nm (Dental Laser System 4 × 4™, General Project Ltd., Montespertoli, Florence, Italy) was carried out as described in detail previously [21]. The irradiation of TiU discs was performed for 1 min in non-contact mode and in continuous (CW) or pulsed (PW) wave operation mode, through a polyamide-coated silica fiber (Ø = 600 μm) positioned perpendicular to the TiU disc surface and kept at a constant distance of about 2–5 mm from the surface. Other laser specification and irradiation parameters are reported in Table 1.

Cell cultures

Human osteoblast-like Saos2 cells from American Type Culture Collection (ATCC; Manassas, VA, USA) were routinely cultured in cell culture plates in growth medium containing F12-Coon's modification medium (Sigma, Milan Italy) supplemented with 10% fetal bovine serum (FBS; Sigma), 1% L-glutamine, and 100 U/ml penicillin-streptomycin (Sigma).

Human bone marrow (*BM*) *mesenchymal stromal cells* (MSCs) were obtained from normal donors from iliac crest and aspirates, cultured and immunophenotypically and morphologically characterized as previously described [25].

Cells were cultured in growth medium containing Dulbecco's modified Eagle's medium (DMEM)

Table 1 Laser specifications

MoModality	Continuous wave (CW)	Pulsed wave (PW)
Frequency (kHz)	N.A.	20
Pulse on duration (μs)	N.A.	7
Duty cycle (%)	N.A.	14
Peak radiant power (W)	N.A.	3.1
Average radiant power (W)	2	0.44
Numeric aperture	0.22	0.22
Beam divergence (deg)	25	25
Target diameter (mm)	6	6
Target area (cm^2)	0.3	0.3
Fluence at target surface (J/cm^2)	400	88

supplemented with 10% FBS, 2 mM L-glutamine, and 100 U/ml penicillin-streptomycin (Sigma).

Experimental group sampling

Both human osteoblast-like Saos2 cells and MSCs were harvested prior to confluence and cultured onto TiU disc surfaces in their specific growth medium. The discs were randomly assigned to one of the following groups:

- *Chlorhexidine digluconate* (*CHX*) *group.* In order to mimic the in vivo peri-implantitis treatment conditions, prior to cell seeding, TiU discs were pre-treated with CHX as follows:

1. 0.2% CHX (Sigma) for 5 min
2. 0.2% CHX for 5 min and gently rinsed with PBS
3. 0.2% CHX for 5 min, gently rinsed with PBS, and air dried for 1 h and 30 min

Given that, CHX local treatment in vivo could also affect the cells around the implant, and in some experiments, the cells were seeded on untreated TiU and cultured for 24 h in growth medium to allow cell adhesion; after that, the discs with the cells were gently washed with PBS and incubated for 5 min with 0.2% CHX solution and then shifted in growth medium for additional 2 and 24 h.

- *Laser group.* Both cell types were cultured onto 808 ± 10 nm GaAlAs diode laser-treated TiU disc surfaces (CW-TiU and PW-TiU) in their specific growth medium for 24 h. To promote osteogenic differentiation, the cells were cultured for 7 and 21 days in their specific growth medium supplemented with 100 μg/ml ascorbic acid, 10 mM β-glycerophosphate, and 10 nM dexamethasone (Sigma). The differentiation medium was replaced every 3–4 days. The cells were seeded on TiU discs immediately after each disc treatment.
- *Control group.* Cells cultured on untreated TiU, on plastic culture plates, or on glass coverslips served as controls.

MTS cell viability assay

Cell viability was determined by 3-(4.5-dimethylthiazol-2-yl)-5-(3-carboxymethoxyphenyl)-2-(4-sulfophenyl)-2Htetrazolium (MTS) assay (Promega Corp., Madison, WI, USA), essentially as previously reported [26]. The optical density (OD) of soluble colored formazan resulting from tetrazolium reduction by mitochondrial enzymes of viable cells was measured using a multi-well scanning spectrophotometer (ELISA reader; Amersham, Pharmacia Biotech, Cambridge, UK) at 492 nm wavelength.

EdU (5-ethynyl-2′-deoxyuridine) incorporation assay

The assay was performed by using the fluorescent Click-iT EdU Cell Proliferation Assay (Life Technologies) according to the manufacturer's instructions. The cells on TiU discs or on glass coverslips were incubated in the presence of the provided solution of 10 μM EdU (24 h), washed with PBS, fixed with 0.5% buffered paraformaldehyde (PFA, 10 min at RT), permeabilized with cold acetone (3 min), and then incubated with the Alexa Fluor 488 EdU detection solution (30 min at RT). The samples were observed under a confocal Leica TCS SP5 microscope (Leica Microsystems, Mannheim, Germany). The number of the cells with EdU positive nuclei was evaluated in 10 random 200 × 200-μm-square microscopic fields (63× ocular) in each cell preparation and expressed as percentage of the total cell number evaluated by labeling nuclei with propidium iodide (PI, 1:30; Molecular Probes). Counting was performed by two different operators in at least three different cell preparations for each experiment; experiments were performed in triplicate.

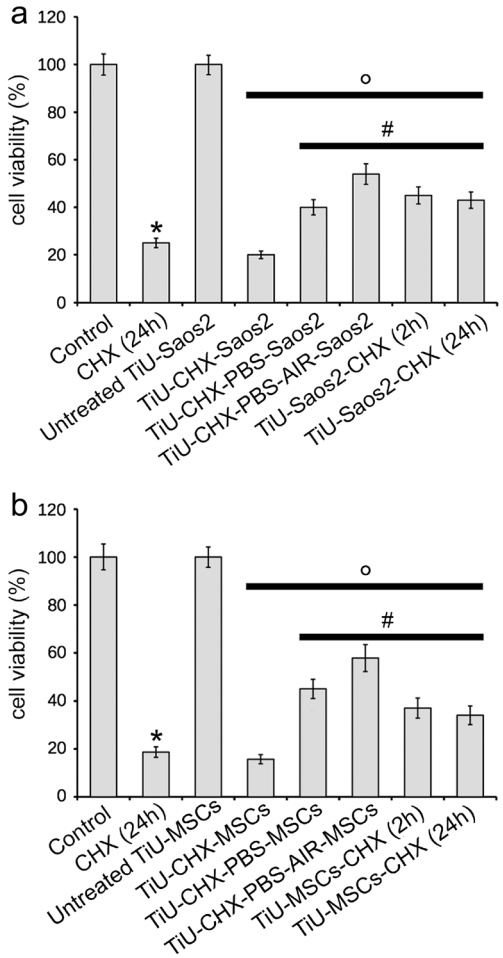

Fig. 1 Effect of CHX on cell viability (MTS assay). Saos2 osteoblasts (**a**) and human bone marrow-derived MSCs (**b**) were seeded on untreated TiU or on TiU pre-treated as follows: (i) with 0.2% CHX for 5 min (TiU-CHX); (ii) with 0.2% CHX for 5 min and gently rinsed with PBS (TiU-CHX-PBS); (iii) with 0.2% CHX for 5 min, gently rinsed with PBS, and air dried for 1 h and 30 min (TiU-CHX-PBS-AIR). The cells were then cultured for 24 h in the cell-specific growth medium. In some experiments, the cells were seeded on untreated TiU discs and cultured for 24 h in growth medium to allow cell adhesion; after that, the discs were incubated for 5 min with 0.2% CHX solution and then shifted in growth medium for additional 2 and 24 h [TiU-Saos2 or MSC-CHX (2 h) or (24 h)]. Control refers to cells cultured on plastic culture plates and CHX (24 h) to the cells on plastic culture plate, treated with 0.2% CHX for 5 min and cultured for 24 h in growth medium. Cell viability of control cells and of cells on untreated TiU corresponded to 100%. Viability of cells subjected to different treatments was expressed as a percentage with respect of that of control cells or cells cultured on untreated TiU. The values are expressed as mean ± S.E.M. obtained from three independent experiments carried out in triplicates. Significance of differences: $^{*}p < 0.05$ vs control; $^{\circ}p < 0.05$ vs Untreated TiU; $^{\#}p < 0.05$ vs TiU-CHX

Confocal laser scanning microscope analysis

Immunofluorescence analysis on fixed cells, on TiU discs, or on glass coverslips was performed essentially as reported previously [26] with the following primary antibodies: rabbit polyclonal anti-Ki67 (1:100; Abcam, Cambridge, UK) or rabbit polyclonal anti-osteopontin (1:50; Santa Cruz Biotechnology, Santa Cruz, CA, USA) primary antibodies. The immunoreactions were revealed by incubation with specific anti-rabbit Alexa Fluor 488-conjugated IgG (1:200; Molecular Probes, Eugene, OR, USA) for 1 h at RT. Actin filament organization was evaluated by labeling the cells with Alexa Fluor 488- or tetramethylrhodamine isothiocyanate (TRITC)-labeled phalloidin (1:100; Sigma). In some experiments, the cells were stained with PI (1:30; Molecular Probes) to reveal nuclei. TiU discs containing the labeled cells were placed in microscopic slides, rehydrated with a drop of water, and observed under a confocal Leica TCS SP5 microscope equipped with a HeNe/Ar laser source for fluorescence measurements and with differential interference contrast (DIC) optics. The glass coverslips containing labeled cells were mounted with an antifade mounting medium (Biomeda Gel mount, Electron Microscopy Sciences, Foster City, CA, USA) before observations. Observations were performed using a Leica Plan Apo 63X/1.43NA oil immersion objective. Series of optical sections (1024 × 1024 pixels each; pixel size 204.3 nm) 0.4 μm in thickness were taken through the depth of the cells at intervals of 0.4 μm. Images were then projected onto a single "extended focus" image. The number of the cells with Ki67-positive nuclei was evaluated in 10 random 200 × 200-μm-square microscopic fields (63× ocular) in each cell preparation and expressed as number of Ki67-positive nuclei *per* optical field. Counting was performed by two different operators in at least three different cell preparations for each experimental condition; experiments were performed in triplicate. Densitometric analysis of the intensity of osteopontin fluorescent signal was performed on digitized images using ImageJ software http://rsbweb.nih.gov/ij) in 20 regions of interest (ROIs) of 100 μm^2 for each confocal stacks (at least 10).

Fluorescent mineralized nodules assay

The evaluation was performed by Fluorescent Osteolmage™ Mineralization assay (Lonza Walkersville, Inc., Walkersville, MD, USA), based on the specific binding of the fluorescent Osteolmage™ staining reagent to the hydroxyapatite portion of the bone-like nodules (Ca^{2+} deposits) deposited by cells, according to the manufacturer's instructions. The cells cultured for 21 days in osteogenic differentiation medium on TiU discs or on glass coverslips were fixed with 0.5% buffered PFA and then incubated with the staining reagent (30 min at RT). Labeled cells were then observed under the confocal laser scanning microscope. Densitometric analysis of mineralized nodule (Ca^{2+} deposits) fluorescent signal intensity was performed on digitized images using ImageJ software http://rsbweb.nih.gov/ij) in 20 regions of interest (ROI) of 100 μm^2 for each confocal stack (at least 10).

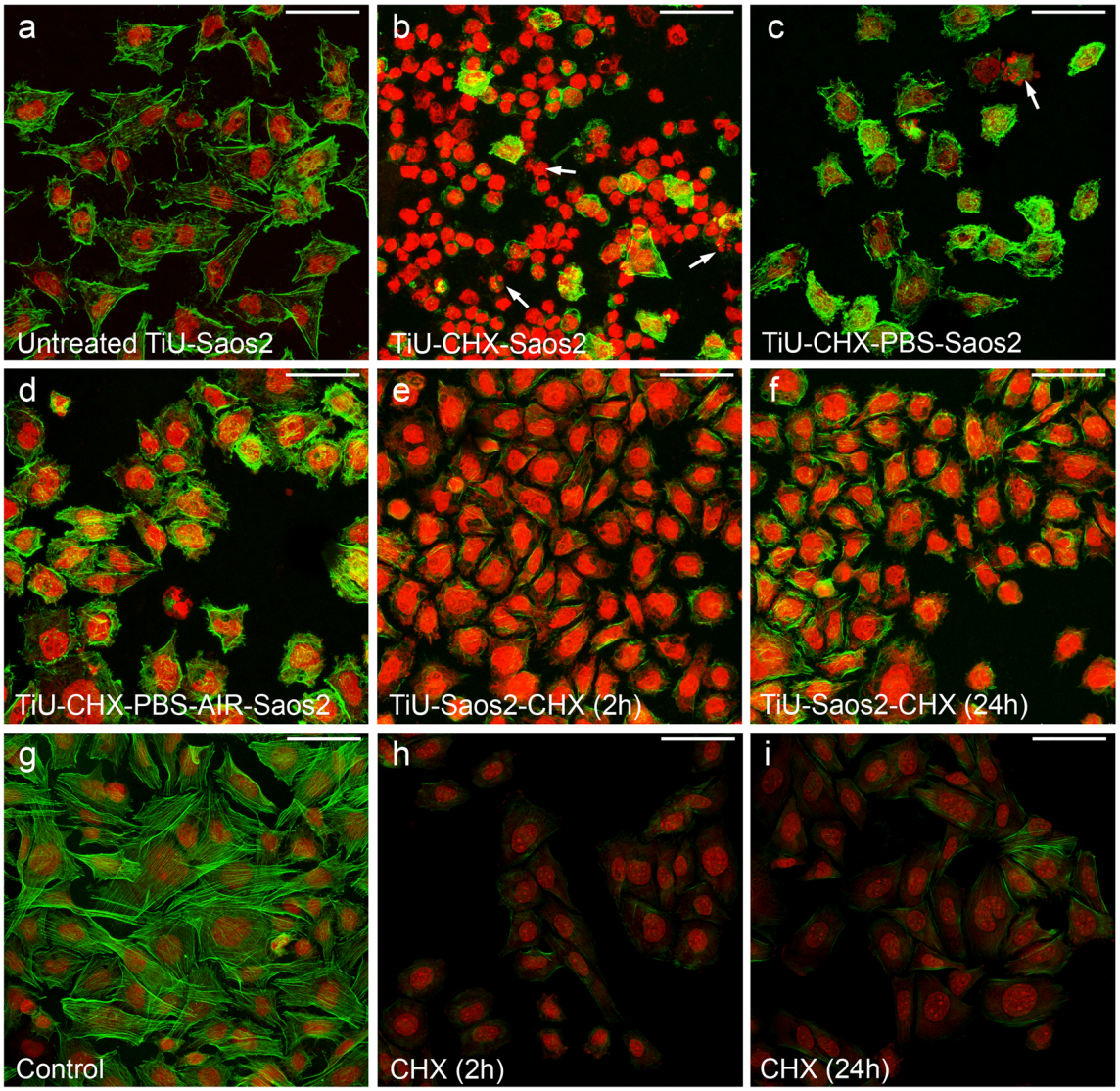

Fig. 2 Effect of CHX on Saos2 osteoblast morphology. Saos2 osteoblasts were seeded on **a** untreated TiU or on TiU pre-treated with **b** 0.2% CHX for 5 min (TiU-CHX-Saos2); **c** 0.2% CHX for 5 min and gently rinsed with PBS (TiU-CHX-PBS-Saos2); and **d** 0.2% CHX for 5 min, gently rinsed with PBS, and air dried for 1 h and 30 min (TiU-CHX-PBS-AIR-Saos2). The cells were then cultured for 24 h in the cell-specific growth medium. **e**, **f** The cells were seeded on untreated TiU and cultured for 24 h in growth medium to allow cell adhesion; after that, the discs were incubated for 5 min with 0.2% CHX solution and then shifted in growth medium for additional **e** 2 h and **f** 24 h [TiU-Saos2-CHX (2 h) or (24 h)]. **g** Control osteoblasts cultured on glass coverslips. **h**, **i** Osteoblasts cultured on glass coverslips treated with 0.2% CHX for 5 min and cultured for 2 h [CHX (2 h)] or 24 h [CHX (24 h)] in growth medium. Fixed cells were stained with PI to reveal nuclei (*red*) and Alexa 488-conjugated phalloidin to detect cytoskeleton actin filaments (*green*) and observed under a confocal laser scanning microscope. *Arrows* in **b** and **c** indicate apoptotic bodies. Scale bar 50 μm. The images are representative of at least three independent experiments performed in triplicate

Statistical analysis

The values are expressed as mean ± standard error of the mean (S.E.M.) obtained from at least three independent experiments carried out in triplicates. Statistical analysis of differences between the experimental groups was performed using one-way ANOVA followed by Newman-Keuls multiple comparison test; results were considered statistically significant if $p < 0.05$. Calculations were performed using the GraphPad Prism 4.0 statistical software (GraphPad, San Diego, CA, USA).

Results

Cell viability and morphological analysis of osteoblasts and MSCs on CHX-treated TiU discs

The results of the MTS cell viability assay showed that both osteoblasts and MSCs cultured on all CHX pre-treated TiU, as indicated in the "*Materials and methods*" section or cultured on untreated TiU and then exposed to CHX, showed a reduced viability as compared to the cells cultured on untreated TiU

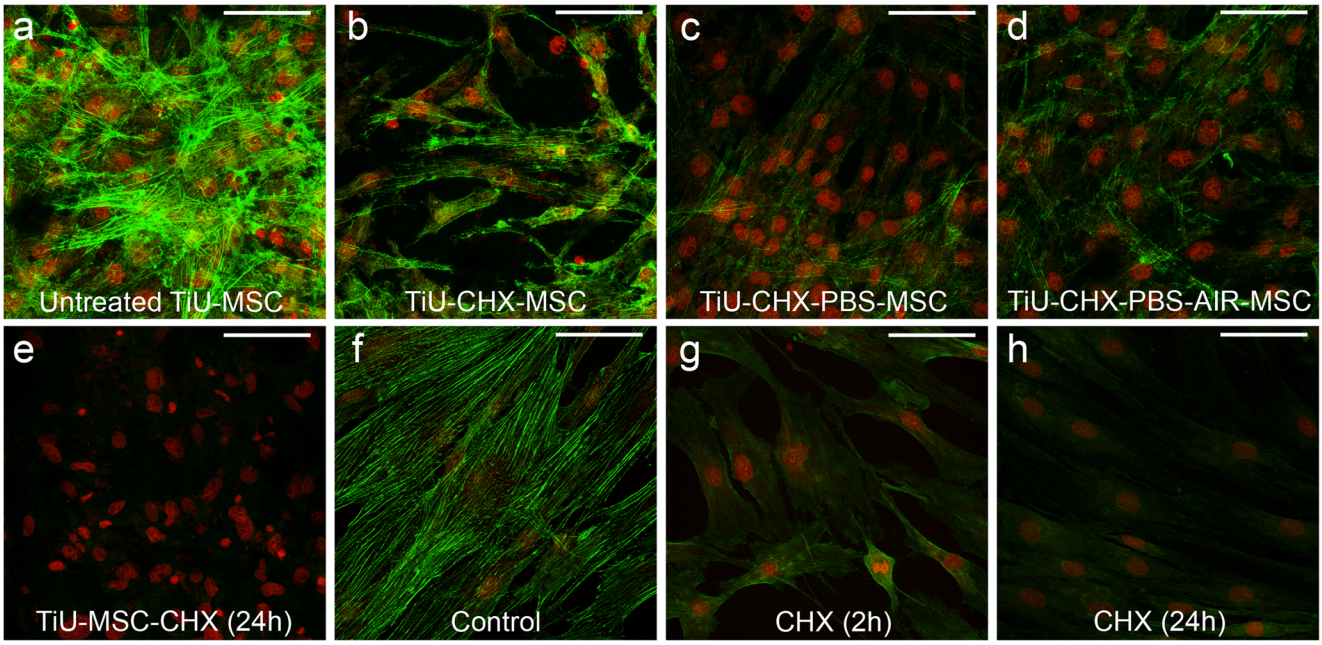

Fig. 3 Effect of CHX on MSC morphology. MSCs were seeded on **a** untreated TiU or on TiU pre-treated with **b** 0.2% CHX for 5 min (TiU-CHX-MSCs); **c** 0.2% CHX for 5 min and gently rinsed with PBS (TiU-CHX-PBS-MSCs); and **d** 0.2% CHX for 5 min, gently rinsed with PBS, and air dried for 1 h and 30 min (TiU-CHX-PBS-AIR-MSCs). The cells were then cultured for 24 h in the cell-specific growth medium. **e** The cells were seeded on untreated TiU and cultured for 24 h in growth medium to allow cell adhesion; after that, the discs were incubated for 5 min with 0.2% CHX solution and then shifted in growth medium for additional 24 h [TiU-MSCs-CHX (24 h)]. **f** Control MSCs cultured on glass coverslips. **g**, **h** MSCs cultured on glass coverslips treated with 0.2% CHX for 5 min and cultured for 2 h [CHX (2 h)] or 24 h [CHX (24 h)] in growth medium. Fixed cells were stained with PI to reveal nuclei (*red*) and Alexa 488-conjugated phalloidin to detect cytoskeleton actin filaments (*green*). Scale bar 50 μm. The images are representative of at least three independent experiments performed in triplicate

(Fig. 1a, b), suggesting a cytotoxic effect of CHX in our experimental conditions. In particular, the higher reduction in cell viability was revealed in the cells seeded on TiU pre-treated with CHX without rinse. A significant reduction of cell viability was also evident when the cells were cultured on glass coverslip and exposed to CHX solution according to our previous data [27]. Reduced viability was associated with dramatic morphological alterations, as judged by confocal laser scanning microscopy analysis of the cells labeled with PI to reveal nuclei and Alexa 488-conjugated phalloidin to stain cytoskeleton actin filaments (Figs. 2 and 3). In particular, we observed that osteoblasts were able to attach to untreated TiU; in fact, the cells were spread over the surface and displayed actin filaments arranged in a web-like structure or in parallel arrays (Fig. 2a) quite similar to those of the control cells on glass coverslips (Fig. 2g). By contrast, osteoblasts cultured on TiU pre-treated with CHX in all conditions showed a robust actin cytoskeleton disarrangement as compared to those on untreated TiU (Fig. 2b–d). In detail, the pre-treatment of TiU with CHX without rinsing displayed the highest cytotoxic effects, likely due to the persistence of the pharmacological agent on the surface and to its direct contact with the cells, able to affect cell adhesion and to induce a massive cell death (Fig. 2b). In fact, some cells showed the typical features of necrotic death (intact nuclei, round shape, actin filament disassembly or disappearance), whereas others displayed signs of apoptosis (apoptotic bodies) (Fig. 2b). CHX-induced cell damage appeared to be attenuated by PBS rinsing (Fig. 2c) and even more by the subsequent air drying (Fig. 2d), but not totally prevented, again suggesting the persistence of the cytotoxic agent on the implant surface. Finally, osteoblasts cultured on TiU discs for 24 h in growth medium, then exposed to 0.2% CHX solution for 5 min, and further cultured for 2 h or

Fig. 4 Cytoskeleton organization and proliferation analysis of osteoblasts and MSCs cultured on 808 ± 10 nm GaAlAs diode laser irradiated-TiU discs. Saos2 osteoblasts and MSCs were cultured for 24 h on untreated TiU discs or on TiU discs irradiated with 808 ± 10 nm GaAlAs diode laser in continuous wave (CW-TiU) or pulsed wave (PW-TiU) modality. **a**, **b** Representative confocal laser scanning microscopy images of osteoblasts **a** stained with Alexa 488-conjugated phalloidin to detect cytoskeleton actin filaments (*green*) and **b** showing nuclear incorporation of EdU (*green*); counterstaining was performed with PI to label nuclei. **c**, **d** Representative confocal laser scanning microscopy images of MSCs **c** immunostained with antibody against Ki67 (*green*) and labeled with TRITC-conjugated phalloidin to detect cytoskeleton actin filaments (*red*) and **d** showing nuclear incorporation of EdU (*green*) and counterstained with PI to reveal nuclei (*red*). **b**, **d** *Yellow-orange color* indicates co-localization between red and green fluorescence signals. Scale bar 50 μm. **e**, **g** Quantitative analysis of EdU positive nuclei of **e** osteoblasts and **g** MSCs, expressed as percentage of the total nuclei number. **f** Quantitative analysis showing the number of Ki67-positive nuclei of MSCs *per* optical field. The data are representative of at least three independent experiments, performed in triplicate. The values are expressed as mean ± S.E.M.

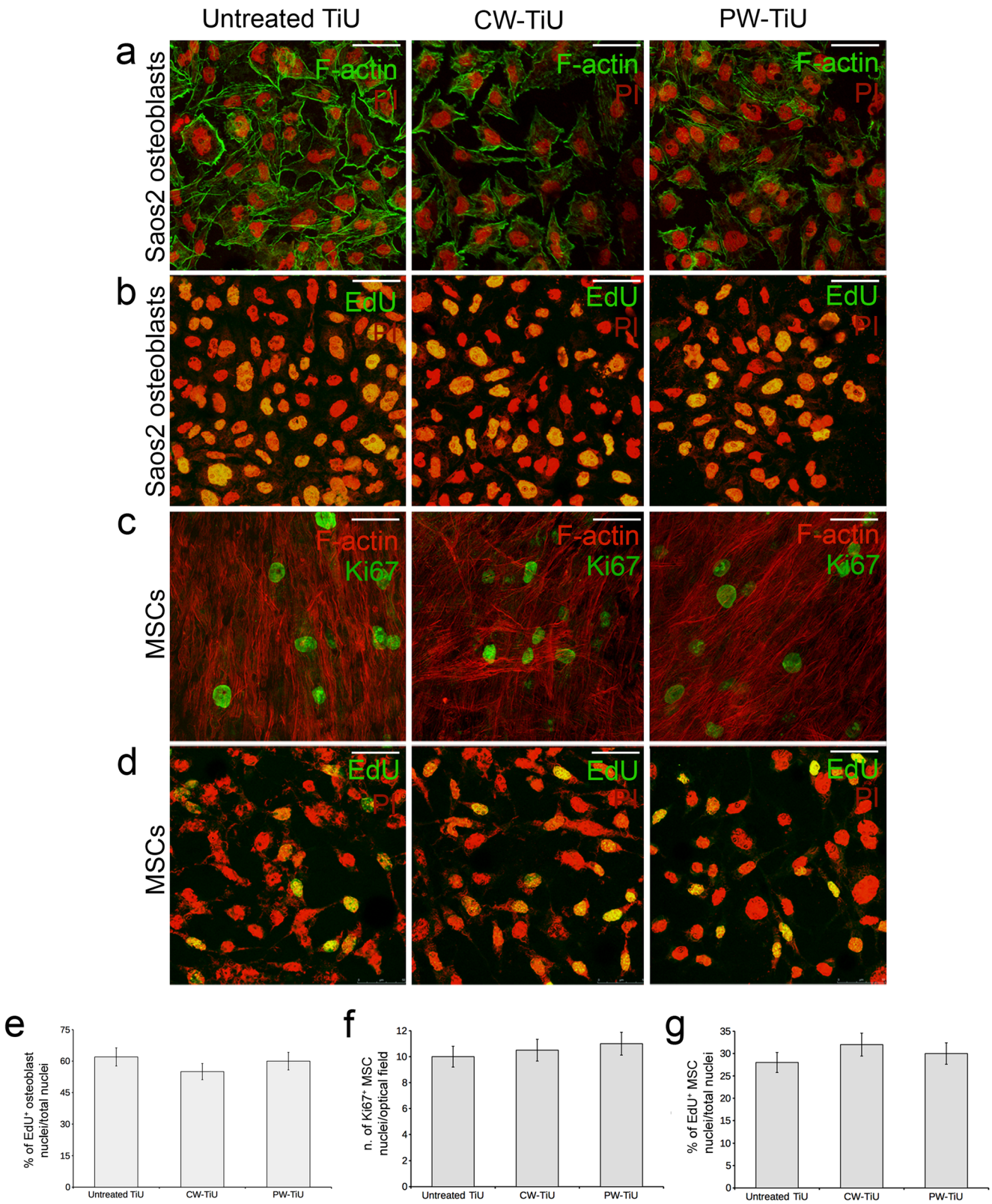

24 h before being fixed showed dramatic morphological alterations as compared to cells on untreated TiU, mainly consisting in actin disarrangement (Fig. 2e, f). The cytotoxicity of CHX, in terms of morphological changes, was confirmed also on osteoblasts cultured on glass coverslips (Fig. 2g–i) according to previously reported data [27]. MSCs on CHX-pretreated discs showed similar morphological alterations as osteoblasts (Fig. 3). In particular, on the untreated

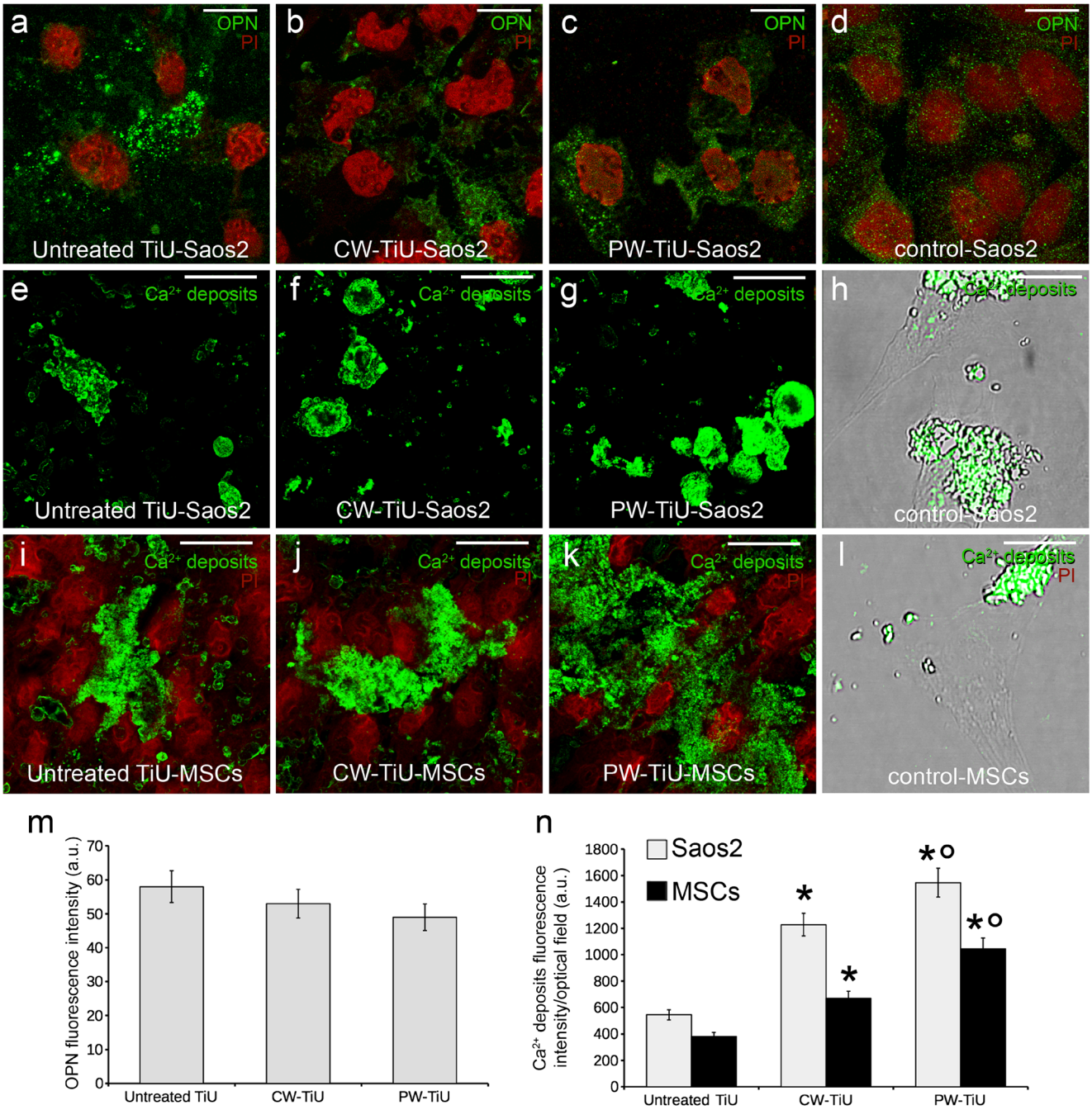

Fig. 5 Confocal fluorescence analysis of osteogenic differentiation. **a**–**d** Representative confocal immunofluorescence images of Saos2 osteoblasts cultured in osteogenic differentiation medium for 7 days on **a** untreated TiU discs or **b**, **c** TiU discs irradiated with 808 ± 10 nm GaAlAs diode laser in **b** continuous wave (CW-TiU-Saos2) or **c** pulsed wave (PW-TiU-Saos2) modality or **d** on glass coverslip (control-Saos2), fixed and stained with antibody against osteopontin (OPN, *green*) and with PI (*red*) to label nuclei. **e**–**l** Representative confocal laser scanning microscope images of **e**–**h** Saos2 osteoblasts and **i**–**l** MSCs cultured for 21 days on **e**, **i** untreated TiU discs or **f**, **g**, **j**, **k** TiU discs irradiated with 808 ± 10 nm GaAlAs diode laser in **f**, **j** CW (CW-TiU) or **g**, **k** PW (PW-TiU) modality or **h**, **l** on glass coverslips (control), fixed and stained with the fluorescent Osteolmage™ staining reagent (*green*) binding the hydroxyapatite portion of the bone-like nodule structures deposited by cells (Ca^{2+} deposits). In **i**–**k**, nuclei were counterstained in red with PI. In **h** and **l**, the confocal fluorescence images are superimposed to DIC images. Scale bar: in **a**–**d**, 20 μm; in **e**–**l**, 30 μm. **m**, **n** Histograms reporting the densitometric analyses of the intensity of the fluorescence signal of **m** OPN and **n** Ca^{2+} deposits performed on digitized images. The data are representative of at least three independent experiments, performed in triplicate. The values are expressed as mean ± S.E.M. Significance of differences: *$p < 0.05$ vs untreated TiU; °$p < 0.05$ vs CW-TiU

TiU discs, the cells displayed well-structured F-actin filaments spanning through the length of the cells (Fig. 3a) which appeared significantly reduced and disarranged in the cells cultured on CHX-treated TiU discs (Fig. 3b). PBS rinse (Fig. 3c) or subsequent air drying (Fig. 3d) was able to reduce CHX-induced damages but not to prevent them. Of note, the treatment with CHX of the cells adhering on TiU, the discs caused the disappearance of cytoskeleton structures, suggesting a high sensitivity of the cells to this agent (Fig. 3e). The cytotoxicity of CHX was confirmed for MSCs cultured on glass coverslip (Fig. 3f–h).

Altogether, these data suggested the cytotoxicity of CHX and the reduced biocompatibility of CHX pre-treated TiU discs with osteoblasts and MSCs.

Osteoblast and MSC responses to 808 ± 10 nm GaAlAs diode laser-irradiated TiU discs

MTS assay revealed that the viability of the cell-cultured TiU surfaces pre-treated with 808 ± 10 nm GaAlAs diode laser in CW or PW mode (CW-TiU and PW-TiU) was comparable to that of cells cultured on untreated TiU discs (OD 492 nm, Saos2 osteoblasts: untreated TiU, 0.459 ± 0.07; CW-TiU, 0.392 ± 0.09; PW-TiU, 0.438 ± 0.05. MSCs: untreated TiU, 0.398 ± 0.06; CW-TiU, 0.407 ± 0.05; PW-TiU, 0.397 ± 0.04. $p > 0.05$). The capability of both cell types to colonize and adhere to CW-TiU and PW-TiU was preserved as evaluated by the morphological analysis at confocal laser scanning microscopy, showing the presence of numerous cells with a well organized and structured cytoskeleton on diode pre-treated discs as on untreated ones (Fig. 4a, c). Moreover, we observed that the cells were also able to undergo proliferation on CW-TiU and PW-TiU. Indeed, the percentage of both osteoblasts (Fig. 4b, e) and MSCs (Fig. 4d, g) with nuclei positive for EdU, a pyrimidine analogue incorporated into the newly synthesized DNA in place of thymidine by the S phase cells, on CW-TiU and PW-TiU, was quite comparable to that on untreated TiU. Unaltered proliferative ability of MSCs on CW-TiU and PW-TiU was further confirmed by confocal immunofluorescence analysis of the expression of Ki67 antigen, a nuclear protein present during all active phases of the cell cycle (G_1, S, G_2, and mitosis) but absent from resting cells (G_0) (Fig. 4c, f).

The results of osteogenic differentiation evaluation assessed by confocal immunofluorescence analysis of the expression of osteopontin, a bone matrix non-collagenous glycophosphoprotein secreted by osteoblasts during bone mineralization and remodeling [28] and by the fluorescent analysis of inorganic hydroxyapatite mineralized nodule formation showed that: (*i*) osteoblasts cultured on CW- or PW-TiU for 7 days in osteogenic differentiation medium expressed osteopontin which appeared punctiform and scattered throughout the cytoplasm similarly to the cells on untreated TiU (Fig. 5a–d, m); (*ii*) both osteoblasts (Fig. 5e–g, n) and MSCs (Fig. 5i–k, n) on CW- or PW-TiU culture for 21 days in osteogenic differentiation medium displayed deposition of mineralized bone-like nodule structures (Ca^{2+} deposits) on implant surface as observed in controls (Fig. 5h, l). Surprisingly, the Ca^{2+} deposit fluorescent signal intensity/optical field related to the cells cultured on CW- and even more on PW-TiU appeared higher than that on untreated TiU suggesting a possible improvement of the osteoinductive properties of these treated surfaces.

Discussion

A necessary condition for the long-term clinical success of dental implant after peri-implantitis treatments is its re-osseointegration, a process critically related to the biological behavior of the cells of soft and hard tissues surrounding implant involved in the restoration the bone support. In particular, re-osseointegration essentially proceeds following the same phases of peri-implant osteogenesis occurring after the first implant placement, which involves different cell types namely mesenchymal cells, pre-osteoblasts, and osteoblasts which, at that site, adhere, proliferate, and differentiate to build bone matrix, leading to biological fixation/anchorage of the device [29]. The occurrence and achievement of implant re-osseointegration following peri-implantitis treatments is a very critical point, and data are still controversial [30, 31]. This is mostly because (*i*) implant surface characteristics including topographical configuration, micro-texture, chemical composition, and physical properties have been demonstrated to be determinant factors for the initial cell response at the cell/material interface, thus ultimately affecting the rate and quality of the de novo tissue [17, 18, 22] and (*ii*) there is still a lack of information about the effect of different peri-implantitis treatments on the biocompatibility of the dental implant surface with the cells of peri-implant tissues [3–8]. On these bases, the results of the present in vitro study appear intriguing and of potential clinical interest. Indeed, they demonstrate that the irradiation of TiU implant surface with GaAlAs diode laser emitting at λ = 808 ± 10 nm operating in CW and PW mode preserved the viability of both tested cell types as well as their capability to colonize the surface and adhere on it. In fact, the cells seeded on the laser pre-treated surfaces showed morphological features similar to those of the cells cultured on untreated TiU with a well-organized cytoskeleton and intact nuclei according with previous observations [17, 32, 33]. We observed also that the cells did not change their proliferation rate on the diode laser-treated surfaces; indeed, the percentage of both osteoblasts and MSC

◀ cells with nuclei positive for the pyrimidine analog EdU or for the Ki67 factor was similar to that of the cells cultured on untreated TiU. Moreover, the osteogenic differentiation experiments indicated that the diode laser treatment of the TiU surfaces did not affect their well-known osteoconductive properties [17, 18, 22]. Osteoblasts and MSCs maintained in fact the capability to undergo osteogenic differentiation as showed by the expression the bone matrix non-collagenous glyco-phosphoprotein osteopontin as well as by the apposition of mineralized bone-like nodules on the treated surface. Of note, data showing an increase of the Ca^{2+} deposit fluorescent signal intensity *per* optical field in the cells cultured on CW- and even more on PW-TiU as compared to those on untreated TiU seemed to suggest the capability of the laser treatment to improve the osteoconductive properties of TiU surface. These data are consistent with previous observations showing that light irradiation of TiO_2 surface may positively influence implant biocompatibility [33–35]. The mechanisms by which laser could exert this action remain still to be elucidated. It can be hypothesized the occurrence of a laser induced-functionalization of titanium similarly to photofunctionalization as previously described [36, 37]: the light could modify the energy or chemical composition of the surface, stimulating the deposition and aggregation of mineralized nodules.

This study demonstrated also the cytotoxicity in vitro of CHX (0.2%), the conventional chemotherapic antiseptic agent used for peri-implantitis treatment [23, 24] both when applied on TiU surface before cell seeding and directly on the cells cultured on the TiU discs, supporting previous data from our research group and others [27, 38–42]. Indeed, in all our experimental conditions for both cell types, CHX treatment induced a drastic reduction of viability as compared to untreated cells associated with dramatic morphological alterations, consisting in the disarrangement of actin cytoskeleton in correlation with the reduced ability of the cells to adhere to the implant surface. Osteoblasts showed also typical features of necrotic death and signs of apoptosis. The fact that the major damage was observed in the osteoblasts cultured on CHX-pretreated TiU surfaces rather than in those cultured on untreated surface subsequently exposed to the antiseptic agent could be explained by the reported data showing that CHX did not alter titanium surface characteristics and was capable of being uptaken, adsorbed, and released by rough TiU surfaces owing to their larger surface area, higher number of binding sites, and micro-cavities [24, 41]. In particular, it has been reported that a higher percentage of the available CHX (in particular applied at the concentration of 0.2%) become adsorbed and slowly released over 24 h, when contacting a rough titanium surface as compared to a smooth surface [41]. If, on one side, such CHX retention by titanium surfaces could raise interest in the antimicrobial action of this chemical agent on implant surfaces, on the other, it is worth to underline that it could impair implant biocompatibility with osteoblasts. In particular CHX could reduce cell substrate adhesion ability likely affecting several matrix components and cell adhesion receptors such as integrin, as previously reported also for other cell types [42–45]. Moreover, it is also reasonable that cells cultured for 24 h on untreated TiU surface before being exposed to the chemotherapic agent can become firmly attached to the surface therefore displaying a reduced susceptibility to the toxic agent. On the other hand, in the latter experimental conditions, MSCs showed a different behavior as compared to osteoblasts; indeed, they displayed the complete disappearance of cytoskeleton, thus suggesting a very high sensitivity of these cells to CHX. However, further investigations are required to clarify this cell response.

In conclusion, the results of this study contribute to provide further experimental evidence for considering the potential of 808 ± 10 nm GaAlAs diode laser at the indicated parameter setting, as a valuable treatment option for tissue peri-implantitis mainly when considering that an ideal clinical treatment should exhibit selective cytotoxicity and maintain a good balance among implant bacterial decontamination and biocompatibility and to discourage the use of CHX. In any case, it must be considered that the present in vitro study has been performed in standardized laboratory conditions using clean discs. Such situation is consistently different from the clinical condition of laser or CHX-aided implant surgery, in which a whole implant, with its global mass and corresponding forces acting on it, interacts with peri-implant tissues and could come in contact with blood, inflammatory cells, and proteins. For this reason, the translation of experimental results to the clinical practice must proceed with a great caution.

Acknowledgements The authors are grateful to Dr. Benedetta Mazzanti (Department of Experimental and Clinical Medicine—Section of Hematology, University of Florence) for providing the human bone marrow MSCs and critically revising the experimental design and manuscript. The titanium discs were kindly provided by Nobel Biocare (Göteborg, Sweden) and Dental Laser System 4 × 4™ laser by General Project, Italy.

Compliance with ethical standards

Conflict of interest The authors declare that they have not conflict of interest.

Ethical approval All procedures performed in studies involving human participants were in accordance with the institutional and/or national research committee and with the 1964 Helsinki Declaration and its later amendments or comparable ethical standards. Local Ethical Committee approval no. prot. 23/2007 was obtained for isolation and collection of bone marrow-derived mesenchymal stromal cells.

Informed consent Informed written consent was signed by all bone marrow donors.

Funding This study was supported by Odontostomatologic Laser Therapy Center Via dell' Olivuzzo 162, 50143, Florence, Italy and by grants from MIUR (Ministero dell'Istruzione dell'Università e della Ricerca—ex Ateneo 60%)—Italy to CS, DN, SZO.

References

1. Albrektsson T, Canullo L, Cochran D, De Bruyn H (2016) "Peri-Implantitis": a complication of a foreign body or a man-made "disease". Facts and fiction. Clin Implant Dent Relat Res 18:840–849. doi:10.1111/cid.12427
2. Sousa V, Nibali L, Spratt D, Dopico J, Mardas N, Petrie A, Donos N (2016) Peri-implant and periodontal microbiome diversity in aggressive periodontitis patients: a pilot study. Clin Oral Implants Res. doi:10.1111/clr.12834
3. Valderrama P, Blansett J, Gonzalez MG, Cantu MG, Wilson TG (2014) Detoxification of implant surfaces affected by peri-implant disease: an overview of non-surgical methods. Open Dental Journal 8:77–84. doi:10.2174/1874210601408010077
4. Yuan K, Chan YJ, Kung KC, Lee TM (2014) Comparison of osseointegration on various implant surfaces after bacterial contamination and cleaning: a rabbit study. Int J Oral Maxillofac Implants 29:32–40. doi:10.11607/jomi.2436
5. Froum SJ, Dagba AS, Shi Y, Perez-Asenjo A, Rosen PS, Wang WC (2016) Successful surgical protocols in the treatment of peri-implantitis: a narrative review of the literature. Implant Dent 25:416–426. doi:10.1097/ID.0000000000000428
6. Htet M, Madi M, Zakaria O, Miyahara T, Xin W, Lin Z, Aoki K, Kasugai S (2016) Decontamination of anodized implant surface with different modalities for peri-implantitis treatment: lasers and mechanical debridement with citric acid. J Periodontol 87:953–961. doi:10.1902/jop.2016.150615
7. Lang MS, Cerutis DR, Miyamoto T, Nunn ME (2016) Cell attachment following instrumentation with titanium and plastic instruments, diode laser, and titanium brush on titanium, titanium-zirconium, and zirconia surfaces. Int J Oral Maxillofac Implants 31:799–806. doi:10.11607/jomi.4440
8. Ouanounou A, Hassanpour S, Glogauer M (2016) The influence of systemic medications on osseointegration of dental implants. J Can Dent Assoc 82:g7
9. Romanos G (2015) Current concepts in the use of lasers in periodontal and implant dentistry. J Indian Soc Periodontol 19:490–494. doi:10.4103/0972-124X.153471
10. Romeo U, Nardi GM, Libotte F, Sabatini S, Palaia G, Grassi FR (2016) The antimicrobial photodynamic therapy in the treatment of peri-implantitis. Int J Dent. doi:10.1155/2016/7692387
11. Natto ZS, Aladmawy M, Levi PA Jr, Wang HL (2015) Comparison of the efficacy of different types of lasers for the treatment of peri-implantitis: a systematic review. Int J Oral Maxillofac Implants 30:338–345. doi:10.11607/jomi.3846
12. Ashnagar S, Nowzari H, Nokhbatolfoghahaei H, Yaghoub Zadeh B, Chiniforush N, Choukhachi ZN (2014) Laser treatment of peri-implantitis: a literature review. J Lasers Med Sci 5:153–162
13. Kreisler M, Götz H, Duschne H (2002) Effect of Nd:YAG, Ho:YAG, Er:YAG, CO2, and GaAIAs laser irradiation on surface properties of endosseous dental implants. Int J Oral Maxillofac Implants 17:202–211
14. Giannelli M, Lasagni M, Bani D (2015) Thermal effects of λ=808 nm GaAlAs diode laser irradiation on different titanium surfaces. Lasers Med Sci 30:2341–2352. doi:10.1007/s10103-015-1801-y
15. Rios FG, Viana ER, Ribeiro GM, González JC, Abelenda A, Peruzzo DC (2016) Temperature evaluation of dental implant surface irradiated with high-power diode laser. Lasers Med Sci 31:1309–1316. doi:10.1007/s10103-016-1974-z
16. Gittens RA, Olivares-Navarrete R, McLachlan T, Cai Y, Hyzy SL, Schneider JM, Schwartz Z, Sandhage KH, Boyan BD (2012) Differential responses of osteoblast lineage cells to nanotopographically-modified, microroughened titanium-aluminum-vanadium alloy surfaces. Biomaterials 33:8986–8994. doi:10.1016/j.biomaterials
17. Kohal RJ, Bächle M, Att W, Chaar S, Altmann B, Renz A, Butz F (2013) Osteoblast and bone tissue response to surface modified zirconia and titanium implant materials. Dent Mater 29:763–776. doi:10.1016/j.dental.2013.04.003
18. Feller L, Jadwat Y, Khammissa RA, Meyerov R, Schechter I, Lemmer J (2015) Cellular responses evoked by different surface characteristics of intraosseous titanium implants. Biomed Res Int. doi:10.1155/2015/171945
19. Mailoa J, Lin GH, Chan HL, MacEachern M, Wang HL (2014) Clinical outcomes of using lasers for peri-implantitis surface detoxification: a systematic review and meta-analysis. J Periodontol 85:1194–1202. doi:10.1902/jop.2014.130620
20. Mettraux GR, Sculean A, Bürgin WB, Salvi GE (2016) Two-year clinical outcomes following non-surgical mechanical therapy of peri-implantitis with adjunctive diode laser application. Clin Oral Implants Res 27:845–849. doi:10.1111/clr.12689
21. Giannelli M, Landini G, Materassi F, Chellini F, Antonelli A, Tani A, Zecchi-Orlandini S, Rossolini GM, Bani D (2016) The effects of diode laser on *Staphylococcus aureus* biofilm and *Escherichia coli* lipopolysaccharide adherent to titanium oxide surface of dental implants. An in vitro study. Lasers Med Sci 31:1613–1619
22. Sharma A, McQuillan AJ, Sharma LA, Waddell JN, Shibata Y, Duncan WJ (2015) Spark anodization of titanium-zirconium alloy: surface characterization and bioactivity assessment. J Mater Sci Mater Med 26:221. doi:10.1007/s10856-015-5555-7
23. Giannelli M, Pini A, Formigli L, Bani D (2011) Comparative in vitro study among the effects of different laser and LED irradiation protocols and conventional chlorhexidine treatment for deactivation of bacterial lipopolysaccharide adherent to titanium surface. Photomed Laser Surg 29:573–580. doi:10.1089/pho.2010.2958
24. Ryu HS, Kim YI, Lim BS, Lim YJ, Ahn SJ (2015) Chlorhexidine uptake and release from modified titanium surfaces and its antimicrobial activity. J Periodontol 86:1268–1275. doi:10.1902/jop.2015.150075
25. Urbani S, Caporale R, Lombardini L, Bosi A, Saccardi R (2006) Use of CFDA-SE for evaluating the in vitro proliferation pattern of human mesenchymal stem cells. Cytotherapy 8:243–253
26. Sassoli C, Chellini F, Squecco R, Tani A, Idrizaj E, Nosi D, Giannelli M, Zecchi-Orlandini S (2016) Low intensity 635 nm diode laser irradiation inhibits fibroblast-myofibroblast transition reducing TRPC1 channel expression/activity: new perspectives for tissue fibrosis treatment. Lasers Surg Med 48:318–332. doi:10.1002/lsm.22441
27. Giannelli M, Chellini F, Margheri M, Tonelli P, Tani A (2008) Effect of chlorhexidine digluconate on different cell types: a molecular and ultrastructural investigation. Toxicol in Vitro 22:308–317
28. Fujihara S, Yokozeki M, Oba Y, Higashibata Y, Nomura S, Moriyama K (2006) Function and regulation of osteopontin in response to mechanical stress. J Bone Miner Res 21:956–964
29. Davies JE (2003) Understanding peri-implant endosseous healing. J Dent Educ 67:932–949
30. Subramani K, Wismeijer D (2012) Decontamination of titanium implant surface and re-osseointegration to treat peri-implantitis: a literature review. Int J Oral Maxillofac Implants 27:1043–1054
31. Meyle J (2012) Mechanical, chemical and laser treatments of the implant surface in the presence of marginal bone loss around implants. Eur J Oral Implantol 5:S71–S81

32. Naddeo P, Laino L, La Noce M, Piattelli A, De Rosa A, Iezzi G, Laino G, Paino F, Papaccio G, Tirino V (2015) Surface biocompatibility of differently textured titanium implants with mesenchymal stem cells. Dent Mater 31:235–243. doi:10.1016/j.dental.2014.12.015
33. Romanos GE, Everts H, Nentwig GH (2000) Effects of diode and Nd:YAG laser irradiation on titanium discs: a scanning electron microscope examination. J Periodontol 71:810–815
34. Terriza A, Díaz-Cuenca A, Yubero F, Barranco A, González-Elipe AR, Gonzalez Caballero JL, Vilches J, Salido M (2013) Light induced hydrophilicity and osteoblast adhesion promotion on amorphous TiO2. J Biomed Mater Res 101:1026–1035. doi:10.1002/jbm.a.34405
35. Allegrini S Jr, Yoshimoto M, Salles MB, de Almeida Bressiani AH (2014) Biologic response to titanium implants with laser-treated surfaces. Int J Oral Maxillofac Implants 29:63–70. doi:10.11607/jomi.3213
36. Lorenzetti M, Dakischew O, Trinkaus K, Lips KS, Schnettler R, Kobe S, Novak S (2015) Enhanced osteogenesis on titanium implants by UVB photofunctionalization of hydrothermally grown TiO_2 coatings. J Biomater Appl 30:71–84. doi:10.1177/0885328215569091
37. Flanagan D (2016) Photofunctionalization of dental implants. J Oral Implantol 42:445–450
38. John G, Becker J, Schwarz F (2014) Effects of taurolidine and chlorhexidine on SaOS-2 cells and human gingival fibroblasts grown on implant surfaces. Int J Oral Maxillofac Implants 29:728–734. doi:10.11607/jomi.2956
39. Park JB, Lee G, Yun BG, Kim CH, Ko Y (2014) Comparative effects of chlorhexidine and essential oils containing mouth rinse on stem cells cultured on a titanium surface. Mol Med Rep 9:1249–1253. doi:10.3892/mmr.2014.1971
40. Vörös P, Dobrindt O, Perka C, Windisch C, Matziolis G, Röhner E (2014) Human osteoblast damage after antiseptic treatment. Int Orthop 38:177–182
41. Kozlovsky A, Artzi Z, Moses O, Kamin-Belsky N, Greenstein RB (2006) Interaction of chlorhexidine with smooth and rough types of titanium surfaces. J Periodontol 77:1194–1200
42. Cline NV, Layman DL (1992) The effects of chlorhexidine on the attachment and growth of cultured human periodontal cells. J Periodontol 63:598–602
43. Röhner E, Hoff P, Gaber T, Lang A, Vörös P, Buttgereit F, Perka C, Windisch C, Matziolis G (2015) Cytokine expression in human osteoblasts after antiseptic treatment: a comparative study between polyhexanide and chlorhexidine. J Investig Surg 28:1–7. doi:10.3109/08941939.2014.941445
44. Ellepola AN, Chandy R, Khan ZU (2016) In vitro impact of limited exposure to subtherapeutic concentrations of chlorhexidine gluconate on the adhesion-associated attributes of oral Candida species. Med Princ Pract 25:355–362. doi:10.1159/000445688
45. Balloni S, Locci P, Lumare A, Marinucci L (2016) Cytotoxicity of three commercial mouthrinses on extracellular matrix metabolism and human gingival cell behaviour. Toxicol in Vitro 34:88–96. doi:10.1016/j.tiv.2016.03.015